Synergistic effect of cAMP and palmitate in promoting altered mitochondrial function and cell death in HepG2 cells

Linxia Zhang[1], **Linsey C. Seitz**[1], **Amy M. Abramczyk**[1], and **Christina Chan**[1,2,*]

[1]Department of Chemical Engineering and Materials Science, Michigan State University, East Lansing, MI 48824

[2]Department of Computer Science and Engineering, Michigan State University, East Lansing, MI 48824

Abstract

Saturated free fatty acids (FFAs), e.g. palmitate, have long been shown to induce toxicity and cell death in various types of cells. In this study, we demonstrate that cAMP synergistically amplifies the effect of palmitate on the induction of cell death in human hepatocellular carcinoma cell line, HepG2 cells. Elevation of cAMP level in palmitate treated cells led to enhanced mitochondrial fragmentation, mitochondrial reactive oxygen species (ROS) generation and mitochondrial biogenesis. Mitochondrial fragmentation precedes mitochondrial ROS generation and mitochondrial biogenesis, and may contribute to mitochondrial ROS overproduction and subsequent mitochondrial biogenesis. Fragmentation of mitochondria also facilitated the release of cytotoxic mitochondrial proteins, such as Smac, from the mitochondria and subsequent activation of caspases. However, cell death induced by palmitate and cAMP was caspase-independent and mainly necrotic.

Keywords

cAMP; palmitate; mitochondria; necrosis; apoptosis

Introduction

Exposure of non-adipose cells, including β-cells, cardiomyocytes and hepatocytes, to excess free fatty acids (FFAs) has been shown to induce lipotoxicity and cell death [1-9]. While elevated unsaturated FFAs, such as oleate and linoleate, are better tolerated, elevated saturated FFAs, such as palmitate, can cause cellular damage and even cell death [1,2]. cAMP (cyclic adenosine monophosphate), an important second messenger, has been shown to protect pancreatic β-cells from palmitate induced apoptosis [10,11]. In addition, cAMP was also reported to protect hepatocytes from bile acid [12,13], Fas ligand [13,14] and TNF-α [13,15] induced apoptosis. Previous study in our group indicated that intracellular cAMP level in HepG2 cells was reduced significantly by palmitate, but not oleate or linoleate [16]. Therefore, we initially hypothesize that the down-regulation of cAMP by palmitate may play a role in the

*To whom correspondence should be addressed:** Christina Chan, Michigan State University, Department of Chemical Engineering and Materials Science, 2527 EB, East Lansing, MI 48824, Tel.: (517) 432-4530, Fax: (517) 432-1105, krischan@egr.msu.edu

Publisher's Disclaimer: This is a PDF file of an unedited manuscript that has been accepted for publication. As a service to our customers we are providing this early version of the manuscript. The manuscript will undergo copyediting, typesetting, and review of the resulting proof before it is published in its final citable form. Please note that during the production process errors may be discovered which could affect the content, and all legal disclaimers that apply to the journal pertain.

induction of cell death. However, restoring cAMP levels in HepG2 cells did not rescue the cells from palmitate-induced toxicity. Moreover, when cAMP level was increased to a high concentration, it synergized with palmitate to promote cell death. cAMP has been proposed as a potential drug target for type 2 diabetes [17], since it appears to enhance insulin secretion. Given that FFAs, which are elevated in obesity and diabetes [18-20], can induce hepatotoxicity, it warrants evaluating the effect of cAMP in the presence of elevated FFAs. In this study, we assess the effect of cAMP on hepatotoxicity and cell death under elevated levels of FFAs.

Mitochondria serve as an integrator for cell death and survival signals [21,22], regulating both apoptosis and necrosis. The onset of mitochondrial membrane permeabilization (MMP) releases a number of cytotoxic proteins, such as cytochrome C and Smac (second mitochondria-derived activator of caspase), from the intermembrane space of mitochondria [23]. Release of these cytotoxic proteins activates both caspase-dependent and independent cell death [23] and such release can be controlled by mitochondrial morphology. In healthy cells, the mitochondria display an elongated and interconnected structure. When a cell becomes apoptotic, its mitochondrial network is disrupted into short and disconnected structure [24,25]. Mitochondrial function is also altered in necrosis, manifesting in diminished mitochondrial ATP production [26]. Apoptosis and necrosis can occur simultaneously in the same cell. Cells in late stage apoptosis may contain necrotic features due to the energy loss and permeabilization of the plasma membrane [27].

Regulation of cell death by mitochondria is intimately tied with generation of reactive oxygen species (ROS) in the mitochondria [28]. Superoxide anion ($O_2^-\cdot$), which is the precursor of most ROS, is primarily generated at Complex I and Complex III in the mitochondria [28]. $O_2^-\cdot$ itself is not a strong oxidant. Dismutation of superoxide by superoxide dismutase (SOD) can produce a stronger oxidant, hydrogen peroxide (H_2O_2), which can be partially reduced to generate one of the strongest oxidants, hydroxyl radical ($HO\cdot$) [29]. Together these oxidants can damage cellular components, proteins and resulted in cell death [29].

This study aims to evaluate how cAMP and FFAs affect hepatocyte survival and death behavior. Our results suggest that a high cAMP level potentiate mitochondrial fragmentation, mitochondrial ROS generation and necrotic cell death initiated by palmitate.

Materials and methods

Cell culture and materials

Human hepatocellular carcinoma cell line HepG2 cells were obtained from American Type Culture Collection. Cells were cultured in DMEM (Dulbecco's modified Eagle's medium) (Invitrogen) containing 10% FBS (fetal bovine serum) (Invitrogen) and 2% PS (Penicillin-Streptomycin) (Invitrogen) at 37°C in 10% CO_2 atmosphere incubator. Saturated free fatty acid palmitate, monounsaturated free fatty acid oleate and polyunsaturated free fatty acid linoleate were purchased from Sigma in the form of sodium salts. These free fatty acids were prepared in medium containing 4% (w/v) fatty acid free BSA (bovine serum albumin) (USBiologicals) at concentration of 0.7 mM. In this study, we used 0.7 mM FFAs concentration since several studies have reported the physiological plasma FFAs level in obese and diabetic patients is around 0.7 mM [18-20]. For palmitate, concentrations of 0.2 mM and 0.4 mM were also prepared. 4% (w/v) BSA in culture medium (medium/BSA) was used as control. 1 μM or 10 μm Forskolin (Sigma), 100 μM isobutylmethylxanthine (IBMX) (Sigma), 1 μM 8CPT-2Me-cAMP (Sigma) and 100 nM glucagon (Sigma) were used to restore cAMP levels. 25 mM N, N'-Dimethylurea (DMU) (Sigma), 100 μg/ml catalase (Sigma), 5 μM Copper (II) 3,5-diisopropylsalicylate (Cu-DIPS) (Sigma) and 50 μM MnTBAP (Biomol) were used as reactive oxygen species scavengers. 10 μM etomoxir (Sigma) was used to inhibit fatty acid oxidation.

Measurement of cytotoxicity

The cytotoxicity of the treatments was measured by release of LDH (lactate dehydrogenase) into the medium according to the manufacture's instructions (Roche Applied Science) as previously described [6]. Briefly, medium was collected after 24 hours. Cells were lysed in 1% Triton-X100 in PBS at 37°C overnight and supernatant was collected. LDH released into medium was denoted as LDH_m, and LDH that was retained in the cells was denoted as LDH_c. LDH activity was measured by the colorimetric assay kit (Roche Applied Science) using plate reader SPECTRAmax plus384 from Molecular Device. Percentage of release was calculated by the following equation: LDH release $\% = LDH_m/(LDH_m+LDH_c)*100$.

cAMP assay

Intracellular cAMP levels were measured by a competitive immunoassay from Assay Designs according to the manufacturer's instructions. In brief, cells were lysed with 0.1 M HCl and supernatants were collected. cAMP in the samples or standards was allowed to bind to a polyclonal cAMP antibody in a competitive manner with alkaline phosphatase-conjugated cAMP. Cleavage of the substrate by the alkaline phosphatase is inversely proportional to the cAMP level in the samples or standards. Colorimetric readings were taken by SPECTRAmax plus384 from Molecular Device at 405 nm. All the readings were normalized to protein level (μg/ml) by bradford assay.

Caspase 3 activity was measured by a kit from BIOMOL according to the manufacture's instructions. Briefly, Cell extracts were incubated with substrate Ac-DEVD-AMC. The cleavage of the substrate will generate fluorescence which is proportional to the concentration of the active caspase 3 in cell extracts. Fluorescence was measured by Spectra MAX GEMINI EM plate reader at excitation of 360 nm and emission of 460 nm. All the readings were normalized to protein levels (μg/ml) by bradford assay.

Measurement of reactive oxygen species (ROS)

Cellular ROS levels were measured using a cell-permeable probe 2′,7′-Dichiorofluorescin diacetate (DCFDA) (Sigma). Cells were loaded with 10 μM DCFDA in PBS for 30 minutes. After washing cells with PBS twice, fluorescence was measured by Spectra MAX GEMINI EM plate reader at excitation of 495 nm and emission of 525 nm. All the readings were normalized to protein levels (μg/ml) by Bradford assay. Mitochondrial superoxide levels were measured using MitoSOX (Invitrogen) mitochondrial superoxide indicator. Cells were loaded with 2.5 μM MitoSOX for 10 minutes at 37°C. After washing cells with PBS twice, fluorescence was measured by Spectra MAX GEMINI EM plate reader at excitation of 510 nm and emission of 580 nm. Mitochondrial superoxide was also detected by confocal microscopy. Similarly, cells cultured in glass-bottom plate (Nunc) were loaded with 2.5 μM MitoSOX for 10 minutes at 37°C and then washed with PBS twice. Fluorescence images were taken with a confocal microscope, Olympus FluoView 1000.

Mitochondria extraction

Mitochondria were extracted using a kit from Pierce. In brief, cells were harvested and washed with PBS once. Reagent A from the kit was added to swell cells on ice. Two minutes later, reagent B was added to lyse the cells. Lysis was carried out by vigorously vortexing every one minute for up to five minutes. Then mitochondria were stabilized by reagent C. Cell suspension was spinned at 700 g for 10 minutes at 4°C to pellet nuclei and cell debris. Supernatant was centrifuged at 12,000 g for 15 minutes at 4°C to pellet mitochondria. Supernatant was saved as cytosolic fraction, and mitochondria pellets were washed and lysed with SDS-PAGE sample buffer.

Western Blot

Mitochondrial-cytosolic extracts were separated by 10% or 16% Tris-HCl gel and transferred to nitrocellulose membrane. Membranes were then blocked in 5% milk in 0.05% Tween-TBS (tris buffered saline) (USB corporation) for one hour and incubated with primary Smac antibody (Cell Signaling), Bcl2 antibody (Cell Signaling) and GAPDH antibody (Cell signaling) overnight at 4°C. Anti-mouse (Pierce) or anti-rabbit (Pierce) HRP-conjugated secondary antibody were added the second day after primary antibody incubation. The blots were incubated for one hour at room temperature and then washed with 0.05% Tween-TBS three times. The blots were visualized by using SuperSignal west femto maximum sensitivity substrate (Pierce).

DNA content and fragmentation

DNA content was measured by labeling DNA with PI (propidium iodide). In brief, harvested cells were fixed with 70% ethanol on ice for 2 hours. RNA was digested by RNase and then DNA was labeled with PI. Labeled samples were measured for DNA contents by flow cytometer BD FACSVantage. Sub-G1 peak was identified as the peak to the left of G0/G1 peak.

Annexin V-PI staining

Apoptosis was measured by the annexin-V-PI (propidium iodide) staining kit (Invitrogen) according to the manufacturer's instructions. Cells were stained with alexa fluor 488 conjugated annexin-V and PI in 1X annexin binding buffer for 15 minute at room temperature and then subjected to flow cytometry analysis by BD FACSVantage. Apoptotic cells were identified as those stained with alexa fluor 488 and showed green fluorescence. Dead cells were those stained with PI and late apoptotic cells were those stained positive for both alexa fluor 488 and PI.

Mitochondria and Smac staining

Mitochondria were labeled using MitoTracker Red (Invitrogen) according to the manufacture's instructions. In brief, cells were incubated with 200 nM MitoTracker Red in warm medium for 30 minutes. Stained cells were washed with warmed PBS and fixed with 3.7% formaldehyde at 37°C for 15 minutes. Cell membrane was pearmeabilized with 2% Triton-X100 for 10 minutes at room temperature. After washing the cells with PBS twice, they were incubated in 1% BSA for 20 minutes at room temperature. Cells were then incubated in anti-mouse Smac primary antibody (Cell Signaling) for 1 hour at room temperature. After washing with PBS three times, cells were incubated in Alexa Fluor-488 conjugated goat anti-mouse secondary antibody for 1 hour at room temperature. Cells were then washed with PBS three times and counterstained with DAPI for 5 minutes. Excess dye was removed by washing and glass coverslips were mounted in ProLong Gold (Invitrogen). Fluorescence images were taken by confocal microscope Olympus FluoView 1000. Percentage of cells with fragmented mitochondria was calculated based on three replicates, with two representative images from each replicate.

Determination of mitochondrial mass

Mitochondrial mass was determined by staining mitochondria with MitoTracker Green FM (Invitrogen). Cells were incubated in 200 nM MitoTracker Green FM in warm medium for 30 minutes and then washed with warm PBS three times to get rid of excess dye. Fluorescence was read by Spectra MAX GEMINI EM plate reader with excitation at 490 nm and emission at 516 nm. Fluorescence was normalized to protein levels (μg/ml) which were measured by bradford assay.

Assessment of triglyceride storage

Triglyceride storage was assessed by Oil Red O staining. Cells were fixed in 3.7% formaldehyde for 30 minutes at room temperature and rinsed with PBS three times (5~10 minutes each time). Cells were rinsed again with water twice. Six parts 0.36% Oil Red O was mixed with four parts deionized water to make Oil Red O working solution. Enough Oil Red O working solution was added into each well and plate was incubated at room temperature for 50 minutes. Excess dye was removed by washing cells with water for three times. Images were taken by Leica RT Color from Diagnostic Instruments. Triglyceride levels were also quantified by an assay from BioVision according to the manufacture's instructions. In brief, samples were collected with 5% Triton-X100. Triglyceride standards and samples were loaded in a 96-well plate. Lipase was then added into each well for 20 minutes at room temperature to convert triglyceride to glycerol and fatty acids. Glycerol is then oxidized in an enzyme mix reaction to generate a product that reacts with the probe, which can then be detected using the colorimetric methods at 570 nm by SPECTRAmax plus384.

Statistical analysis

Statistical analysis were carried out by an unpaired, two tail student T-test. * indicates $p < 0.05$, ** indicates $p < 0.01$ and *** indicates $p < 0.001$.

Results

Palmitate induced cell death in HepG2 cells

Previous work had ascribed a lipotoxic effect to saturated FFAs, i.e. palmitate [1,2]. We evaluated the effect of palmitate as well as unsaturated FFAs, oleate and linoleate, on HepG2 cells. The toxicity, as indicated by LDH release, was observed in palmitate-treated but not oleate- and linoleate treated HepG2 cells (Fig. 1A). In addition, cell staining with propidium iodide (PI, labels dead cells and late apoptotic cells) and Alexa Fluor 488-conjugated annexin V (labels early and late apoptotic cells) indicated that palmitate treatment significantly increased the necrotic (PI positive and annexin V negative) and late apoptotic cell populations (PI positive and annexin V positive) (Fig. 1B). Linoleate also increased the necrotic cell population but much less than with palmitate treatment (Fig. 1B). Palmitate treatment did not affect the population of early apoptotic cells, which was slightly increased in the oleate and linoleate conditions (Fig. 1B).

Palmitate dose dependently reduce intracellular cAMP levels

Previously we showed that intracellular cAMP level was reduced by palmitate but not oleate or linoleate in HepG2 cells [16]. The effect of palmitate on cAMP levels was also dependent on the palmitate concentration. cAMP level was increased slightly by 0.2 mM palmitate and significantly by 0.4 mM palmitate, whereas a high concentration of palmitate (0.7 mM) decreased cAMP level significantly (Fig. 2A). Since the high concentration palmitate caused significant cell death, we assessed whether restoring cAMP level to near control level would prevent cell death. Intracellular cAMP levels were restored by IBMX (phosphodiesterase inhibitor), forskolin (adenylyl cyclase agonist), 8CPT-2Me-cAMP (cell-permeant cAMP analog) and glucagon (a hormone that activates adenylyl cyclase). 100 μM IBMX, 1 μM forsolin, 1 μM 8CPT-2Me-cAMP and 100 nM glucagon restored cAMP levels to near control level in the 0.7 mM palmitate condition (Fig. 2B). A combination of 10 μM forskolin and 100 μM IBMX was also evaluated, which achieved an even higher level of cAMP (Fig. 2B).

cAMP and palmitate synergistically promote cell death at high concentrations

Studies in β-cells indicated that apoptosis was reduced upon supplementation with cAMP increasing agents [10]. However, another study suggested that although apoptosis was reduced,

the mode of cell death was switched to necrosis upon cAMP elevation in the palmitate condition [11]. When we used IBMX, forskolin, 8CPT-2Me-cAMP or glucagon to restore cAMP levels to the control level, the mode and level of cell death remained unchanged in the 0.7 mM palmitate conditions (Fig. 3A). However, when cAMP was increased to a high level by supplementing with forskolin and IBMX (abbreviated as FI), it caused a significant increase in the necrotic cell population (Fig 3A). When the same concentration of FI was used to co-treat cells in control, 0.4 mM palmitate, 0.7 mM palmitate or 0.7 mM oleate, the synergistic increase in necrotic cell death was not observed (Fig 3B).

The increase in the sub-G1 population attests further to the synergistic effect of elevated palmitate concentration and cAMP on cell death. Small fragmented DNA can be washed out from cells, leaving a sub-G1 peak to the left of the G0/G1 peak [30]. Compared with the control cells (Fig. 4A), cells treated with 0.7mM palmitate had a small population of sub-G1 cells (Fig. 4C). The addition of FI increased the sub-G1 population (Fig. 4D), suggestive of further DNA fragmentation, in palmitate but not in the control cells (Fig. 4B). Cells in different cell cycle phases, including sub-G1 cells, were quantified and shown in Fig. 4E. Significant increase in sub-G1 phase cells was already observed 12 hours after 0.7mM palmitate treatment. The synergistic or additive effect of cAMP in promoting DNA fragmentation in the palmitate culture was not observed at 12 hours, (Fig. 4E). However at 24 hours, cAMP increased the sub-G1 fraction significantly in the palmitate condition (Fig. 4E). Although palmitate alone decreased the G2/M phase cells, the addition of FI did not reduce the S phase or G2/M phase cells but rather increased the G2/M phase cells at 12 hours (Fig. 4E). Since cAMP did not prevent cell cycle progression, the increase in cell death caused by cAMP in the palmitate condition is not likely the result of DNA-damage induced cell cycle arrest at the checkpoint.

cAMP and palmitate induced cell death is not caused by palmitate β-oxidation

Mitochondria are the main sites for fatty acid β-oxidation, with acetyl-CoA as one of the primary products. The majority of acetyl-CoA enters the TCA cycle, whereas a small proportion will undergo ketogenesis in the mitochondria matrix [31]. Unused FFAs can be stored in the form of triglyceride in the cytosol. The capacity of non-adipose cells to store FFAs as triglyceride is limited. A previous study indicated that storage of oleate as triglyceride protected non-adipose cells from lipotoxicity, whereas palmitate was poorly incorporated into triglyceride and therefore led to apoptosis [32]. When we measured the level of triglycerides in HepG2 cells, we found that oleate and linoleate were more likely to be stored as triglyceride than palmitate (Fig. 5A, 5B, 5C and 5D). This is in accordance with our previous finding that oxidation is higher with palmitate than with the unsaturated FFAs [16]. Given that the mitochondria serve as primary sites for FFA β-oxidation, enhanced palmitate oxidation may be related to enhanced mitochondrial biogenesis. Therefore we measured the mitochondria mass and found a significant increase in the 0.7 mM palmitate condition (Fig. 6A). Although 0.7 mM greatly enhanced mitochondrial biogenesis in the palmitate treatment, this effect was not observed in the oleate treatment (Fig. 6A). This could be due to the higher ability of oleate to be stored as triglycerides [37]. However, the addition of FI stimulated mitochondrial biogenesis, regardless of the treatment condition (Fig. 6A). This effect was most obvious in the co-treatment of FI with 0.7 mM palmitate (Fig. 6A). Since mitochondria are the primary sites for FFA β-oxidation and cAMP promoted mitochondrial biogenesis to a greater extent in palmitate, we expected that the addition of FI would enhance FFAs β-oxidation and reduce triglyceride storage. However, supplementing FI in the control and the different FFAs did not appear to give a visual difference in triglyceride levels according to Oil Red O staining for triglycerides (Fig. 5E, 5F, 5G and 5H). For further confirmation, we quantified the triglyceride levels. Indeed, supplementing with FI did not change the triglyceride levels (Fig. 5I). It appears that mitochondrial biogenesis did not further enhance FFA β-oxidation. The lower triglyceride level in the palmitate condition was already apparent at 5 and 12 hours after treatment

(Supplementary Fig. S1), whereas mitochondrial biogenesis occurred at a much later time point (Fig. 6B), indicating that β-oxidation occurred prior to mitochondrial biogenesis.

Palmitate was oxidized to a higher extent than oleate and caused significant cell death in HepG2 cells, therefore we assessed whether inhibiting palmitate β-oxidation would reduce or prevent cell death. When the FFAs oxidation inhibitor etomoxir was employed, it did not affect the cell death observed in palmitate, as reported previously [33]. Etomoxir decreased the necrotic population only slightly in the palmitate supplemented with FI condition (Fig. 5J), suggesting that cell death induced by palmitate and palmitate supplemented with FI was not due to β-oxidation.

cAMP synergized with palmitate to alter mitochondria morphology and integrity

Mitochondria are not only primary sites for FFA β-oxidation, but also play an important role in cell death and survival [34]. In healthy cells, mitochondria exhibit elongated and connected morphology. When cells are subjected to apoptotic stimuli, mitochondria fragment into small and disconnected mitochondria [24,25]. Control HepG2 cells exhibited long and connected thread-like mitochondria structure (Fig. 7A). When the cells were subjected to 0.7 mM palmitate treatment, the mitochondria morphology changed dramatically. The interconnected network was disrupted and collapsed into short disconnected morphology (Fig. 7C). The elongated mitochondria network also condensed and collapsed to the perinuclear locations (Fig. 7C, arrow heads). The addition of FI to the control cells did not alter the connectivity of the mitochondria network (Fig. 7B, arrows), however supplementing the palmitate medium with FI continued the disconnected and punctuate mitochondria structure (Fig. 7D, arrow heads) in a higher population of cells (Fig. 7E). No mitochondrial fragmentation was observed in the 0.2 mM palmitate condition (Supplementary Fig. S2B, arrows). When palmitate concentration was increased to 0.4 mM, mitochondrial fragmentation had begun to occur and a number of cells had disconnected and punctuate mitochondria structure (Supplementary Fig. S2C, arrow heads), whereas the majority of cells still have elongated mitochondria network as indicated by the arrow (Supplementary Fig. S2C). As the palmitate concentration was further increased to 0.7 mM, more cells showed short and disconnected mitochondria structures (Supplementary Fig. S2D). Fragmentation of mitochondria is associated with cell death and the release of cytotoxic proteins that reside in the intermembrane space [24]. In accordance with the mitochondrial fragmentation observed in the high palmitate condition, we detected less Smac in the mitochondria and relatively more Smac in the cytosol (Supplementary Fig. S3). Indeed, Smac colocalized in the mitochondria in the control (Fig. 7F) and control supplemented with FI conditions (Fig. 7G), since almost no green fluorescence was observed outside the mitochondria. However more cytosolic Smac (indicated by the green fluorescence) was released into the cytosol in the palmitate (Fig. 7H) and palmitate supplemented with FI conditions (Fig. 7I), suggesting that the mitochondrial membrane integrity was compromised. We also observed that the mitochondrial anti-apoptotic protein Bcl2 level was further reduced by FI supplementation (Supplementary Fig. S3). Bcl2 is an anti-apoptotic protein that antagonizes pro-apoptotic proteins, such as Bax, thereby preventing the release of cytotoxic proteins from the mitochondria [22]. The significant decrease in mitochondrial Bcl2 protein induced by the addition of FI to palmitate treated cells may disrupt the outer mitochondria membrane integrity [35]. As a consequence, cytotoxic proteins, such as Smac which promotes caspase activation by inhibiting the inhibitor of apoptosis (IAP), are more likely to be released into the cytosolic compartment [22]. In support, caspase 3 activity was highest in the palmitate supplemented with FI condition (Fig. 8A), which had the highest level of mitochondrial fragmentation (Fig. 7E) and lowest level of mitochondrial Bcl2 (Supplementary Fig. S3).

Since caspase 3 activity was activated by 0.7 mM palmitate and significantly increased by FI supplementation (Fig. 8A), we assessed whether caspase was involved in causing the cell death.

When the pan caspase inhibitor Z-VAD-FMK was used to inhibit caspase activity, late apoptosis and necrosis were not reduced (Fig. 8B), suggesting that the cell death induced by palmitate and cAMP was caspase-independent. This is not too surprising given that the majority of the population under this condition is necrotic as opposed to apoptotic.

cAMP synergized with palmitate to enhance ROS generation in mitochondria

Mitochondria are also the primary sites for ROS generation. Although palmitate β-oxidation was not the cause of cell death, generation of ROS at Complex I and Complex III during the process of oxidative phosphorylation through the electron transport chain in the mitochondria can induce cell death [28]. Excessive ROS generation can result in cellular damage and cell death. Mitochondrial superoxide anion ($O_2^-\cdot$) was increased significantly in the palmitate condition after 24 hours (Fig. 9B) as compared with the control (Fig. 9A). Moreover, the short, disconnected and perinuclear mitochondria appeared to have higher $O_2^-\cdot$ levels (Fig. 9B, arrow heads). Quantification of mitochondrial $O_2^-\cdot$ levels indicated that palmitate did not induce an increase in mitochondrial $O_2^-\cdot$ levels at 5 or 12 hour, but a significant increase was observed at 24 hours (Fig. 9C). Elevating cAMP level by FI synergistically increased the mitochondrial $O_2^-\cdot$ levels at 24 hours (Fig. 9C). $O_2^-\cdot$ is the precursor of stronger ROS, such as hydrogen peroxide (H_2O_2) and hydroxyl radical (HO·) [28]. When whole cell ROS levels were measured, higher ROS activity was detected in the palmitate condition 24 hours after treatment (Fig. 9D). Similar to the mitochondrial superoxide levels, the cellular ROS level did not increase at 5 and 12 hours. However at 24 hours, FI induced a slight increase in ROS level in the palmitate condition albeit not significantly (Fig. 9D).

In order to evaluate whether ROS production contributes to the cell death induced by palmitate and palmitate supplemented with FI, we used several ROS scavengers. The ROS scavengers employed were: DMU for hydroxyl radicals, catalase for hydrogen superoxide, Cu-DIPS and MnTBAP for superoxide. Employing DMU or catalase resulted in a decrease in both late apoptotic cells and necrotic cells caused by palmitate, however, the decrease was not significant (Fig. 9E). When DMU and catalase were used simultaneously, both late apoptosis and necrosis were reduced significantly in the palmitate condition (Fig. 9E). Similarly, DMU and catalase together significantly reduced late apoptosis and necrosis in palmitate supplemented with FI. DMU itself also significantly reduced both late apoptosis and necrosis but catalase only significantly reduced necrosis (Fig. 9E). The superoxide scavengers Cu-DIPS and MnTBAP did not decrease cell death (data not shown). This is likely due to the reduction of $O_2^-\cdot$ by Cu-DIPS and MnTBAP to generate the stronger ROS, H_2O_2 and HO· [28] which would be expected to further continue the damage to the cells. Although the H_2O_2 and HO· scavengers reduced cell death, H_2O_2 and HO· are not likely the reason that cell death was initiated. At 5 and 12 hours of palmitate and palmitate supplemented with FI treatment, cell death had already been initiated (Supplementary Fig. S4) but the ROS level did not increase until 24 hours (Fig. 9D). However, ROS generation may be linked to mitochondrial fragmentation. At 12 hours, some cells already had fragmented mitochondria in the 0.7mM palmitate condition (Supplementary Fig. S5A, arrow heads). This is especially the case for the cells with fragmented nucleus (Supplementary Fig. S5B, rectangle), their mitochondria were all short and disconnected (Supplementary Fig. S5C, arrow heads). The short and disconnected mitochondria tend to have higher ROS levels (Fig. 9B, arrow heads). Therefore, mitochondria fragmentation precedes ROS generation and may have contributed to the ROS produced.

Discussion

Lipotoxicity induced by palmitate has been demonstrated in a number of different cell types. In human HepG2 cells, both apoptotic behaviors, such as caspase 3 activation (Fig. 8A) and annexin V labeling for phosphatidylserine (Fig. 1B), and necrotic behaviors, such as propidium

iodide (PI) penetration (Fig. 1B), have been observed for palmitate-induced cell death. Many obese and diabetic patients have high plasma FFAs levels [18-20]. cAMP has been proposed as a potential drug target for type 2 diabetes [17] due to it ability to stimulate pancreatic β-cell insulin secretion. Given that elevated FFAs can induce hepatotoxicity, it warrants evaluating the effect of cAMP under the circumstance of high FFAs. In this study, we evaluated the effect of cAMP on hepatotoxicity and cell death under elevated FFAs conditions. A high cAMP level achieved by adding 10 μM forskolin and 100 μM IBMX (abbreviated as FI) promoted palmitate-induced cell death in a synergistic manner (Fig. 3 and 4). The increase in cell death caused by cAMP supplementation was mostly necrotic (Fig. 3B), without an increase in the early apoptotic population (Supplementary Fig. S4), and further appeared to be caspase-independent (Fig. 8B).

Lipotoxicity caused by palmitate may be related to its lower ability to be stored in the form of triglyceride [32]. Reduced cytoxicity and cell death in HepG2 cells was achieved by inhibiting NADH dehydrogenase (complex I), which was accompanied by enhanced triglyceride storage [36]. While oleate and linoleate are more likely to be stored as triglyceride (Fig. 5B and 5C), palmitate was less likely to be stored in the form of triglycerides (Fig. 5D and 5I). The lower ability of palmitate to be stored as triglyceride may contribute to its enhanced oxidation in mitochondria. Indeed, our previous study showed that palmitate was oxidized more than oleate and linoleate by the HepG2 cells [16]. The total mitochondrial mass was increased significantly in the palmitate condition but not in the oleate condition (Fig. 6A). Since mitochondria are the primary sites for FFA β-oxidation, we initially assumed that the induction of mitochondrial biogenesis would allow more palmitate to undergo β-oxidation and therefore have less triglyceride to be stored. cAMP can promote mitochondrial biogenesis by directly regulating mitochondrial related genes or indirectly by inducing the expression of transcriptional coactivator, PGC-1α [37]. When FI was added to the different conditions, mitochondrial biogenesis was enhanced in all cases, but the extent was much higher in the palmitate condition (Fig. 6A). However, the addition of FI did not cause a significant change in triglyceride levels (Fig. 5I). A time-dependent study indicated that mitochondrial biogenesis occurred later than triglyceride storage (Fig. 6B and Supplementary Fig. S1), indicating that mitochondrial biogenesis would not likely contribute to reduced triglyceride storage in the palmitate condition. Therefore, even though FI increased mitochondrial biogenesis (Fig. 6A), triglyceride levels were not affected (Fig. 5I). Since the palmitate condition had higher β-oxidation [16] and lower triglyceride storage (Fig. 5I), we assessed whether palmitate β-oxidation is involved in palmitate-induced cell death. When β-oxidation was inhibited by etomoxir, no change in cell death was observed (Fig. 5J), suggesting that palmitate β-oxidation was not the cause of cell death.

Although β-oxidation was not the cause of cell death, generation of ROS by oxidative phosphorylation through the mitochondrial electron transport chain can damage cells [36]. Indeed, inhibiting NADH dehydrogenase (complex I), one of the primary sites for ROS generation, reduced the cytotoxicity induced by palmitate treatment [36]. Superoxide ($O_2^-\cdot$), which is the precursor of most ROS, was much higher in the palmitate condition and further increased upon FI supplementation (Fig. 9C). In addition to mitochondrial $O_2^-\cdot$ levels, total cellular ROS levels were also much higher in the palmitate condition (Fig. 9D).

Mitochondrial $O_2^-\cdot$ levels correlated with mitochondrial biogenesis (Fig. 6B and 9C). Whether mitochondrial biogenesis promote mitochondrial $O_2^-\cdot$ generation or mitochondrial $O_2^-\cdot$ generation promote mitochondrial biogenesis still remains a question. From our results, it is unlikely that mitochondrial biogenesis itself promoted mitochondrial $O_2^-\cdot$ generation, since FI supplementation promoted mitochondrial biogenesis in the control and oleate conditions (Fig. 6A) but no increase in mitochondrial $O_2^-\cdot$ levels was observed in these two conditions (supplementary Fig. S6). It is possible that $O_2^-\cdot$ generation may enhance mitochondrial

biogenesis. Previous studies have suggested that ROS can enhance nuclear respiratory factor-1 (NRF-1) and mitochondrial transcription factor A (Tfam), which are involved in regulating mitochondrial biogenesis [38,39].

Generation of ROS, however, may be linked to mitochondrial fragmentation. A previous study has indicated that changes in mitochondrial morphology resulted in ROS overproduction [40]. We showed that palmitate induced morphological changes in the mitochondria, causing long interconnected networks (Fig. 7A) to become short disconnected structures located in the perinuclear (Fig. 7C). When HepG2 cells were subjected to palmitate and FI, mitochondrial fragmentation was further enhanced (Fig. 7D), judging by the increase in the total number of cells with fragmented mitochondria (Fig. 7E). Under the conditions of high percent of mitochondrial fragmentation, mitochondrial $O_2^-\cdot$ and total cellular ROS levels were also high (Fig. 9C and 9D). The occurrence of mitochondrial fragmentation precedes mitochondrial ROS generation. At 12 hours, mitochondrial fragmentation had already begun to occur in the 0.7 mM palmitate condition (Supplementary Fig. S5), while ROS generation was not much higher than control until after 12 hours (Fig. 9D). In addition, the fragmented mitochondria tend to have higher superoxide ($O_2^-\cdot$) levels as denoted by the arrow heads in Fig. 9B. Thus it is likely that mitochondrial fragmentation contributed to ROS overproduction. ROS overproduction, in turn, further damages the mitochondria, and as a self defense mechanism, damaged mitochondria stimulates the synthesis of new mitochondria to ameliorate the damage [41]. However, what regulates mitochondrial fragmentation still remains an open question. Recent work in our lab indicated that endoplasmic reticulum (ER) stress was observed several hours after palmitate treatment (unpublished data). ER stress can induce the release of Ca^{2+} from the ER [42]. Release of Ca^{2+} can activate the Ca^{2+} and calmodulin-dependent phosphatase calcineurin [43]. Calcineurin has been shown to dephosphorylate dynamin-related protein 1 (Drp1), a key protein involved in mitochondria fragmentation, and promote mitochondrial fragmentation [44]. Therefore, it is possible that palmitate, which has been shown to induce ER stress [45], initiated Ca^{2+} release and activated calcineurin, which subsequently activates Drp1 and leads to mitochondrial fragmentation.

In summary, cAMP promoted cell death in the presence of high level of palmitate in a synergistic or additive manner in HepG2 cells. The many effects exerted by palmitate on the mitochondria, such as mitochondrial fragmentation, mitochondrial ROS generation, and mitochondrial biogenesis, were amplified by cAMP supplementation. Mitochondrial fragmentation appears to precede ROS generation and may have contributed to mitochondrial ROS overproduction, which in turn stimulated mitochondrial biogenesis.

Supplementary Material

Refer to Web version on PubMed Central for supplementary material.

Acknowledgments

References

[1]. Eitel K, Staiger H, Brendel MD, Brandhorst D, Bretzel RG, Haring HU, Kellerer M. Different role of saturated and unsaturated fatty acids in beta-cell apoptosis. Biochem Biophys Res Commun 2002;299:853–856. [PubMed: 12470657]

[2]. Morgan NG, Dhayal S, Diakogiannaki E, Welters HJ. The cytoprotective actions of long-chain monounsaturated fatty acids in pancreatic beta-cells. Biochem Soc Trans 2008;36:905–908. [PubMed: 18793159]

[3]. Kong JY, Rabkin SW. Palmitate-induced apoptosis in cardiomyocytes is mediated through alterations in mitochondria: prevention by cyclosporin A. Biochim Biophys Acta 2000;1485:45–55. [PubMed: 10802248]

[4]. Ostrander DB, Sparagna GC, Amoscato AA, McMillin JB, Dowhan W. Decreased cardiolipin synthesis corresponds with cytochrome c release in palmitate-induced cardiomyocyte apoptosis. J Biol Chem 2001;276:38061–38067. [PubMed: 11500520]

[5]. Wei Y, Wang D, Topczewski F, Pagliassotti MJ. Saturated fatty acids induce endoplasmic reticulum stress and apoptosis independently of ceramide in liver cells. Am J Physiol Endocrinol Metab 2006;291:E275–281. [PubMed: 16492686]

[6]. Srivastava S, Chan C. Hydrogen peroxide and hydroxyl radicals mediate palmitate-induced cytotoxicity to hepatoma cells: relation to mitochondrial permeability transition. Free Radic Res 2007;41:38–49. [PubMed: 17164177]

[7]. Feldstein AE, Werneburg NW, Canbay A, Guicciardi ME, Bronk SF, Rydzewski R, Burgart LJ, Gores GJ. Free fatty acids promote hepatic lipotoxicity by stimulating TNF-alpha expression via a lysosomal pathway. Hepatology 2004;40:185–194. [PubMed: 15239102]

[8]. Ji J, Zhang L, Wang P, Mu YM, Zhu XY, Wu YY, Yu H, Zhang B, Chen SM, Sun XZ. Saturated free fatty acid, palmitic acid, induces apoptosis in fetal hepatocytes in culture. Exp Toxicol Pathol 2005;56:369–376. [PubMed: 15945276]

[9]. Malhi H, Bronk SF, Werneburg NW, Gores GJ. Free fatty acids induce JNK-dependent hepatocyte lipoapoptosis. J Biol Chem 2006;281:12093–12101. [PubMed: 16505490]

[10]. Kwon G, Pappan KL, Marshall CA, Schaffer JE, McDaniel ML. cAMP Dose-dependently prevents palmitate-induced apoptosis by both protein kinase A- and cAMP-guanine nucleotide exchange factor-dependent pathways in beta-cells. J Biol Chem 2004;279:8938–8945. [PubMed: 14688288]

[11]. Welters HJ, Diakogiannaki E, Mordue JM, Tadayyon M, Smith SA, Morgan NG. Differential protective effects of palmitoleic acid and cAMP on caspase activation and cell viability in pancreatic beta-cells exposed to palmitate. Apoptosis 2006;11:1231–1238. [PubMed: 16703263]

[12]. Webster CR, Anwer MS. Cyclic adenosine monophosphate-mediated protection against bile acid-induced apoptosis in cultured rat hepatocytes. Hepatology 1998;27:1324–1331. [PubMed: 9581687]

[13]. Cullen KA, McCool J, Anwer MS, Webster CR. Activation of cAMP-guanine exchange factor confers PKA-independent protection from hepatocyte apoptosis. Am J Physiol Gastrointest Liver Physiol 2004;287:G334–343. [PubMed: 15044179]

[14]. Fladmark KE, Gjertsen BT, Doskeland SO, Vintermyr OK. Fas/APO-1(CD95)-induced apoptosis of primary hepatocytes is inhibited by cAMP. Biochem Biophys Res Commun 1997;232:20–25. [PubMed: 9125131]

[15]. Li J, Yang S, Billiar TR. Cyclic nucleotides suppress tumor necrosis factor alpha-mediated apoptosis by inhibiting caspase activation and cytochrome c release in primary hepatocytes via a mechanism independent of Akt activation. J Biol Chem 2000;275:13026–13034. [PubMed: 10777606]

[16]. Srivastava S, Zhang L, Jin R, Chan C. A novel method incorporating gene ontology information for unsupervised clustering and feature selection. PLoS ONE 2008;3:e3860. [PubMed: 19052637]

[17]. Furman B, Pyne N, Flatt P, O'Harte F. Targeting beta-cell cyclic 3′5′ adenosine monophosphate for the development of novel drugs for treating type 2 diabetes mellitus. A review. J Pharm Pharmacol 2004;56:1477–1492. [PubMed: 15563754]

[18]. Woerle HJ, Popa E, Dostou J, Welle S, Gerich J, Meyer C. Exogenous insulin replacement in type 2 diabetes reverses excessive hepatic glucose release, but not excessive renal glucose release and impaired free fatty acid clearance. Metabolism 2002;51:1494–1500. [PubMed: 12404204]

[19]. Boden G, Chen X, Capulong E, Mozzoli M. Effects of free fatty acids on gluconeogenesis and autoregulation of glucose production in type 2 diabetes. Diabetes 2001;50:810–816. [PubMed: 11289046]

[20]. Skowronski R, Hollenbeck CB, Varasteh BB, Chen YD, Reaven GM. Regulation of non-esterified fatty acid and glycerol concentration by insulin in normal individuals and patients with type 2 diabetes. Diabet Med 1991;8:330–333. [PubMed: 1677322]

[21]. Goldenthal MJ, Marin-Garcia J. Mitochondrial signaling pathways: a receiver/integrator organelle. Mol Cell Biochem 2004;262:1–16. [PubMed: 15532704]

[22]. Newmeyer DD, Ferguson-Miller S. Mitochondria: releasing power for life and unleashing the machineries of death. Cell 2003;112:481–490. [PubMed: 12600312]

[23]. Saelens X, Festjens N, Vande Walle L, van Gurp M, van Loo G, Vandenabeele P. Toxic proteins released from mitochondria in cell death. Oncogene 2004;23:2861–2874. [PubMed: 15077149]

[24]. Cereghetti GM, Scorrano L. The many shapes of mitochondrial death. Oncogene 2006;25:4717–4724. [PubMed: 16892085]

[25]. Perfettini JL, Roumier T, Kroemer G. Mitochondrial fusion and fission in the control of apoptosis. Trends Cell Biol 2005;15:179–183. [PubMed: 15817372]

[26]. Golstein P, Kroemer G. Cell death by necrosis: towards a molecular definition. Trends Biochem Sci 2007;32:37–43. [PubMed: 17141506]

[27]. Zong WX, Thompson CB. Necrotic death as a cell fate. Genes Dev 2006;20:1–15. [PubMed: 16391229]

[28]. Orrenius S, Gogvadze V, Zhivotovsky B. Mitochondrial oxidative stress: implications for cell death. Annual review of pharmacology and toxicology 2007;47:143–183.

[29]. Turrens JF. Mitochondrial formation of reactive oxygen species. The Journal of physiology 2003;552:335–344. [PubMed: 14561818]

[30]. Darzynkiewicz Z, Juan G, Li X, Gorczyca W, Murakami T, Traganos F. Cytometry in cell necrobiology: analysis of apoptosis and accidental cell death (necrosis). Cytometry 1997;27:1–20. [PubMed: 9000580]

[31]. Garrett, RH.; Grisham, CM. Biochemistry. Brooks/Cole-Thomson Learning; Pacific Grove, CA: 1999.

[32]. Listenberger LL, Han X, Lewis SE, Cases S, Farese RV Jr. Ory DS, Schaffer JE. Triglyceride accumulation protects against fatty acid-induced lipotoxicity. Proc Natl Acad Sci U S A 2003;100:3077–3082. [PubMed: 12629214]

[33]. Srivastava S, Chan C. Application of metabolic flux analysis to identify the mechanisms of free fatty acid toxicity to human hepatoma cell line. Biotechnology and bioengineering 2008;99:399–410. [PubMed: 17615559]

[34]. Green DR, Reed JC. Mitochondria and apoptosis. Science 1998;281:1309–1312. [PubMed: 9721092]

[35]. Cory S, Adams JM. The Bcl2 family: regulators of the cellular life-or-death switch. Nat Rev Cancer 2002;2:647–656. [PubMed: 12209154]

[36]. Srivastava S, Li Z, Yang X, Yedwabnick M, Shaw S, Chan C. Identification of genes that regulate multiple cellular processes/responses in the context of lipotoxicity to hepatoma cells. BMC genomics 2007;8:364. [PubMed: 17925029]

[37]. Hock MB, Kralli A. Transcriptional control of mitochondrial biogenesis and function. Annual review of physiology 2009;71:177–203.

[38]. Perez-de-Arce K, Foncea R, Leighton F. Reactive oxygen species mediates homocysteine-induced mitochondrial biogenesis in human endothelial cells: modulation by antioxidants. Biochemical and biophysical research communications 2005;338:1103–1109. [PubMed: 16259958]

[39]. Miranda S, Foncea R, Guerrero J, Leighton F. Oxidative stress and upregulation of mitochondrial biogenesis genes in mitochondrial DNA-depleted HeLa cells. Biochemical and biophysical research communications 1999;258:44–49. [PubMed: 10222232]

[40]. Yu T, Robotham JL, Yoon Y. Increased production of reactive oxygen species in hyperglycemic conditions requires dynamic change of mitochondrial morphology. Proc Natl Acad Sci U S A 2006;103:2653–2658. [PubMed: 16477035]

[41]. Shen X, Zheng S, Thongboonkerd V, Xu M, Pierce WM Jr. Klein JB, Epstein PN. Cardiac mitochondrial damage and biogenesis in a chronic model of type 1 diabetes. American journal of physiology 2004;287:E896–905. [PubMed: 15280150]

[42]. Deniaud A, Sharaf el dein O, Maillier E, Poncet D, Kroemer G, Lemaire C, Brenner C. Endoplasmic reticulum stress induces calcium-dependent permeability transition, mitochondrial outer membrane permeabilization and apoptosis. Oncogene 2008;27:285–299. [PubMed: 17700538]

[43]. Rusnak F, Mertz P. Calcineurin: form and function. Physiol Rev 2000;80:1483–1521. [PubMed: 11015619]

[44]. Cribbs JT, Strack S. Reversible phosphorylation of Drp1 by cyclic AMP-dependent protein kinase and calcineurin regulates mitochondrial fission and cell death. EMBO Rep 2007;8:939–944. [PubMed: 17721437]

[45]. Karaskov E, Scott C, Zhang L, Teodoro T, Ravazzola M, Volchuk A. Chronic palmitate but not oleate exposure induces endoplasmic reticulum stress, which may contribute to INS-1 pancreatic beta-cell apoptosis. Endocrinology 2006;147:3398–3407. [PubMed: 16601139]
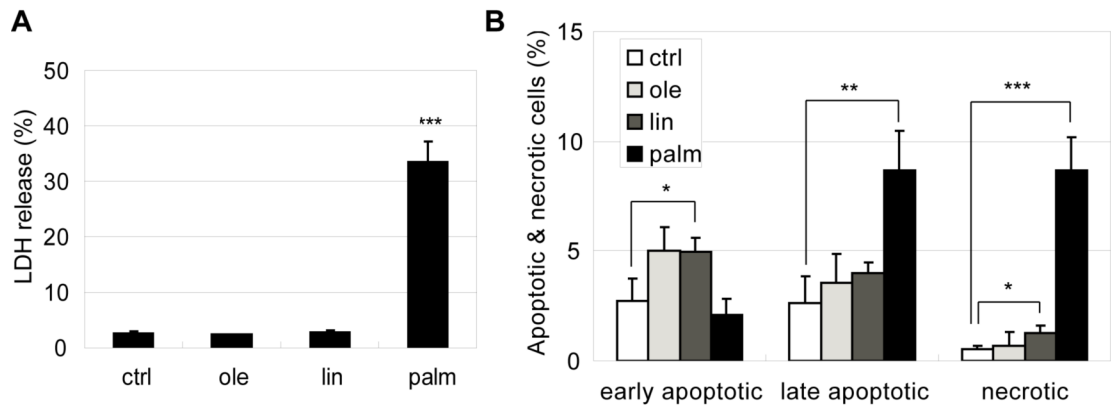
Fig. 1.
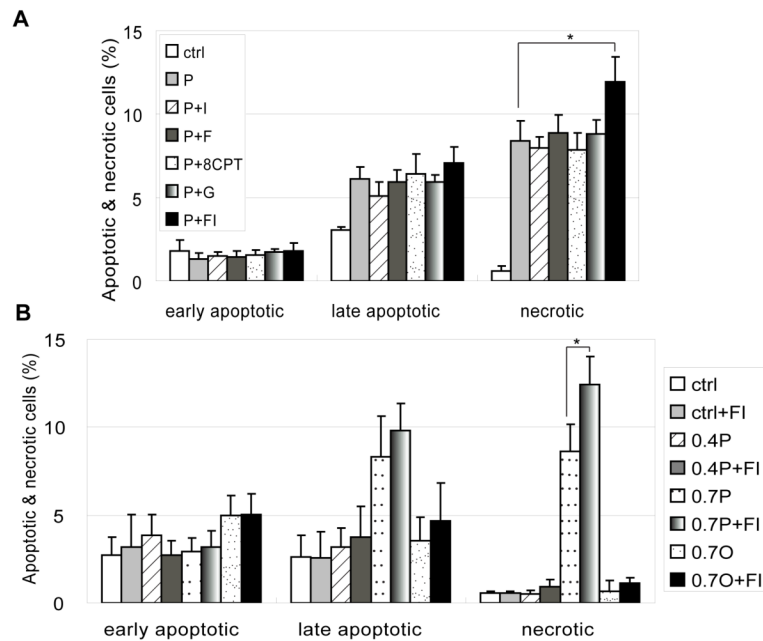(A) LDH release from cells in medium/BSA (ctrl), 0.7 mM oleate, linoleate and palmitate for 24 hrs. (B) Apoptotic and necrotic labeling by PI (propidium iodide) and Alexa Fluor-488 conjugated annexin V for cells in medium/BSA (ctrl), 0.7 mM oleate, linoleate and palmitate for 24 hrs. *Early apoptotic cells:* PI⁻ annexin V⁺ cells; *late apoptotic cells*: PI⁺ annexin V⁺ cells; *necrotic cells*: PI⁺ annexin V⁻ cells (n=3). *: $p < 0.05$; **: $p < 0.01$; ***: $p < 0.001$.
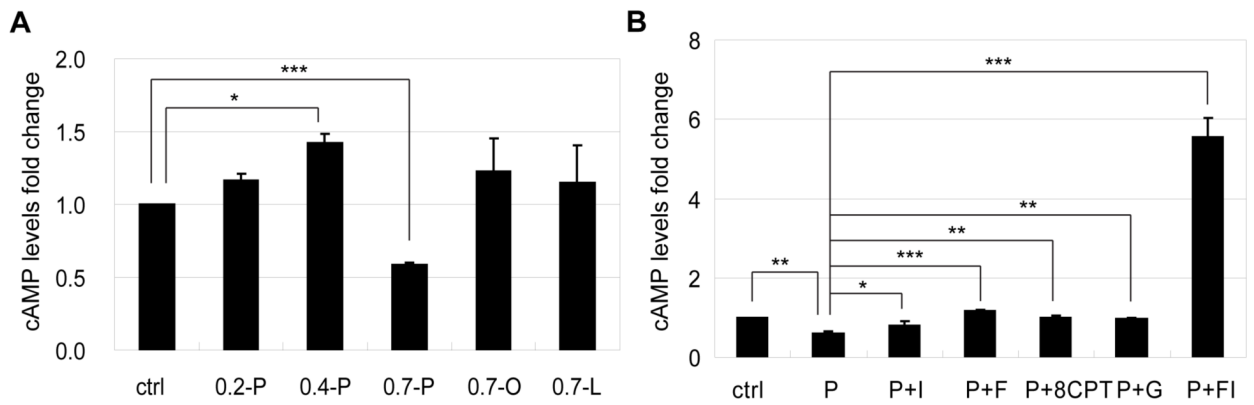
Fig. 2.
(A) Intracellular cAMP levels of cells in control, 0.2 mM palmitatate (0.2-P), 0.4 mM palmitatate (0.4-P), 0.7 mM palmitatate (0.7-P), 0.7 mM oleate (0.7-O) and 0.7 mM linoleate (0.7-L) for 24 hrs (n=4). (B) Intracellular cAMP levels of cells in control, 0.7 mM palmitatate (P), 0.7 mM palmitatate supplemented with 100 μM IBMX (P+I), 0.7 mM palmitatate supplemented with 1 μM forskolin (P+F), 0.7 mM palmitatate supplemented with 1 μM 8CPT-2Me-cAMP (P+8CPT), 0.7 mM palmitatate supplemented with 100 nM glucagon (P+G) and 0.7 mM palmitatate supplemented with 10 μM forskolin and 100 μM IBMX (P+FI) for 24 hrs (n=3). *: p<0.05; **: p<0.01; ***: p<0.001.

Fig. 3.
(A) Apoptotic and necrotic labeling by PI (propidium iodide) and Alexa Fluor-488 conjugated annexin V for cells in control, 0.7 mM palmitatate (P), 0.7 mM palmitatate supplemented with 100 μM IBMX (P+I), 0.7 mM palmitatate supplemented with 1 μM forskolin (P+F), 0.7 mM palmitatate supplemented with 1 μM 8CPT-2Me-cAMP (P+8CPT), 0.7 mM palmitatate supplemented with 100 nM glucagon (P+G) and 0.7 mM palmitatate supplemented with 10 μM forskolin and 100 μM IBMX (P+FI) for 24 hrs. *Early apoptotic cells:* PI$^-$ annexin V$^+$ cells; *late apoptotic cells*: PI$^+$ annexin V$^+$ cells; *necrotic cells*: PI$^+$ annexin V$^-$ cells (n=3). (B) Apoptotic and necrotic labeling by PI (propidium iodide) and Alexa Fluor-488 conjugated annexin V for cells in control, control supplemented with FI (ctrl+FI), 0.4 mM palmitate (0.4P), 0.4 mM palmitate supplemented with FI (0.4P+FI), 0.7 mM palmitate (0.7P), 0.7 mM palmitate supplemented with FI (0.7P+FI), 0.7 mM oleate (0.7O) and 0.7 mM oleate supplemented with FI (0.7O+FI) for 24 hrs (n=3).
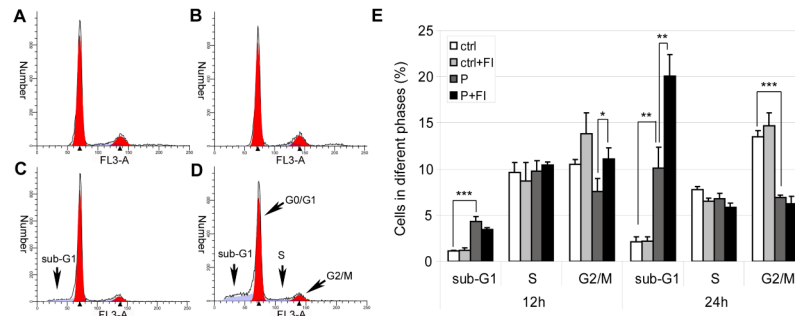
Fig. 4.
Cell cycle analysis of cells treated with desired medium. (A) In control for 24 hrs (ctrl). (B) In control supplemented with 10 μM forskolin and 100 μM IBMX (FI) for 24 hrs (ctrl+FI). (C) In 0.7 mM palmitate for 24 hrs (P). (D) In 0.7 mM palmitate supplemented with FI for 24 hrs (P+FI). (E) Quantification of cells in sub-G1, S and G2/M phases 12 hrs and 24 hrs after treatment (n=3). *: p<0.05; **: p<0.01; ***: p<0.001.
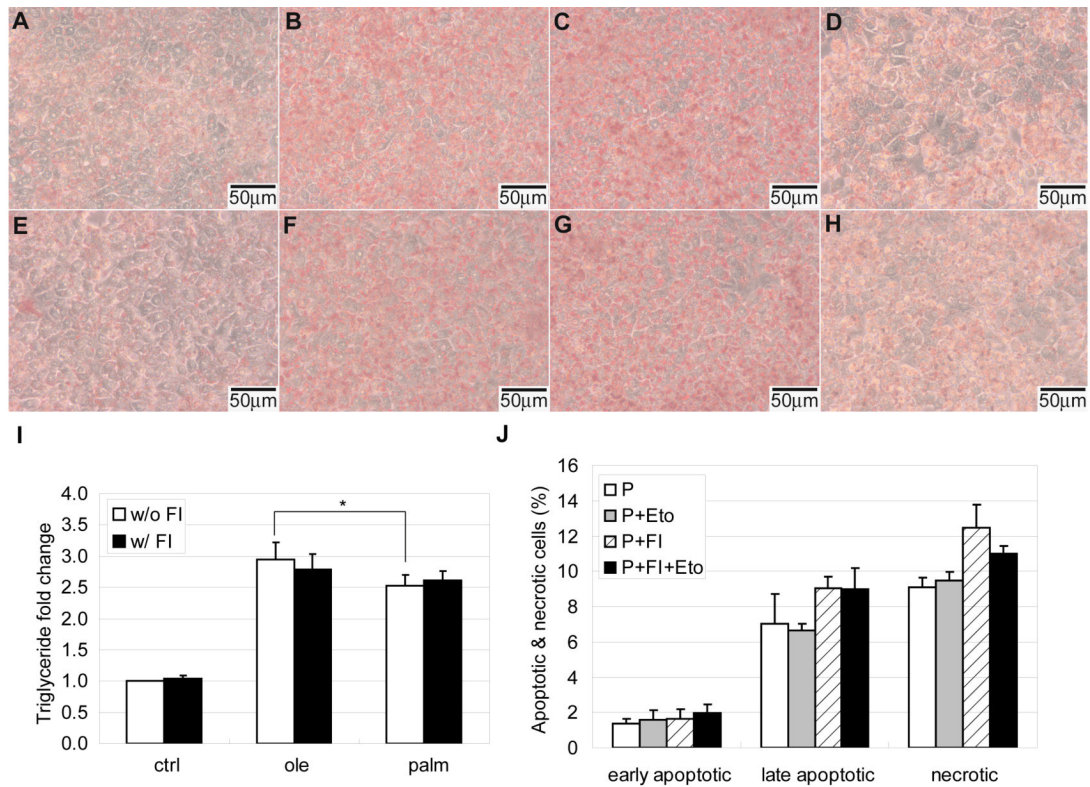
Fig. 5.
(A-H) Triglyceride storage by Oil Red O staining for cells in (A) control, (B) 0.7 mM oleate, (C) 0.7 mM linoleate, (D) 0.7 mM palmitate, (E) control supplemented with 10 μM forskolin and 100 μM IBMX (FI), (F) 0.7 mM oleate supplemented with FI, (G) 0.7 mM linoleate supplemented with FI and (H) 0.7 mM palmitate supplemented with FI for 24 hrs (n=3). (I) Quantification of triglyceride levels by an assay for cells in control, 0.7 mM oleate and 0.7 mM palmitate without (w/o) or with (w/) FI for 24 hrs (n=4). (J) Apoptotic and necrotic labeling by PI (propidium iodide) and Alexa Fluor-488 conjugated annexin V for cells in 0.7 mM palmitate and 0.7 mM palmitate supplemented with FI in the absence or presence of free fatty acid oxidation inhibitor etomoxir (n=3). *: $p<0.05$.
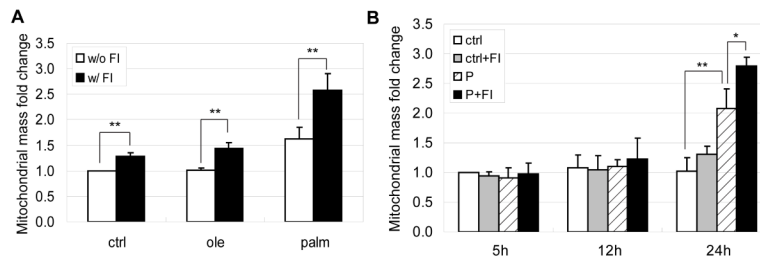
Fig. 6.
(A) Mitochondrial mass fold change of cells in control, 0.7 mM oleate and 0.7 mM palmitate without (w/o) or with (w/) 10 μM forskolin and 100 μM IBMX (FI) for 24 hrs (n=3). (B) Mitochondrial mass fold change of cells in control and 0.7 mM palmitate without (w/o) or with (w/) FI for 5 hrs, 12 hrs and 24 hrs (n=3). *: p<0.05; **: p<0.01.
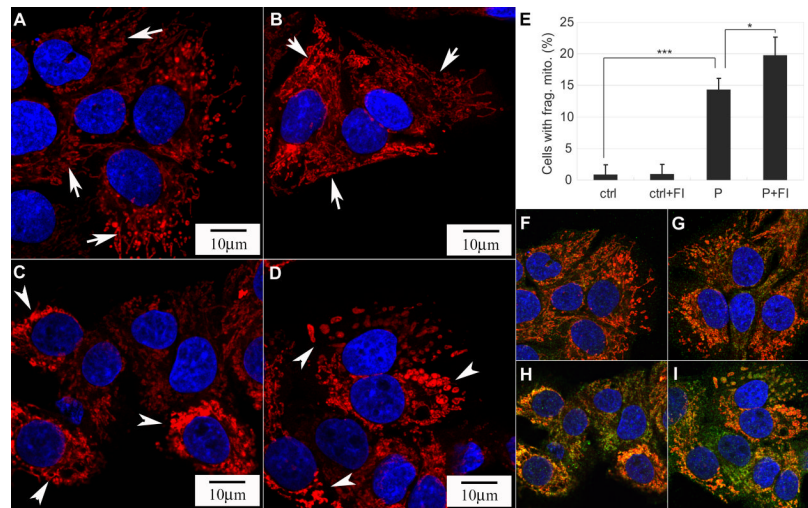
Fig. 7.
(A-D) Mitochondrial morphology of cells in (A) control, (B) control supplemented with 10 μM forskolin and 100 μM IBMX (FI), (C) 0.7 mM palmitate and (D) 0.7 mM palmitate supplemented with FI for 24 hrs (n=3). (A-B) exhibited elongated and tubular structure, while (C-D) displayed short and disconnected morphology. (E) Quantification of the percentage of cells with fragmented mitochondria as displayed in (A-D) (n=3). *: p<0.05; ***: p<0.001. (F-I) Immunostaining of mitochondria (red), Smac (green) and nucleus (blue) for cells in (F) control, (G) control supplemented with FI, (H) 0.7 mM palmitate and (I) 0.7 mM palmitate supplemented with FI for 24 hrs (n=3).
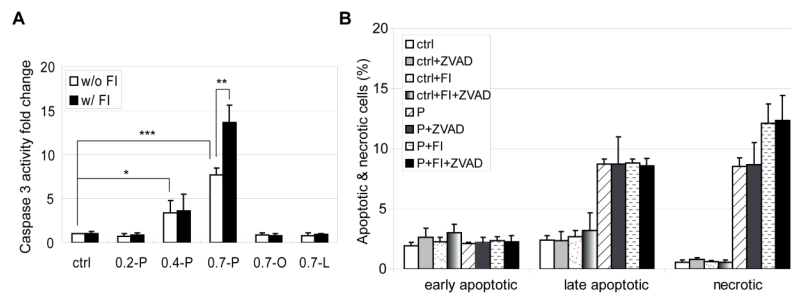
Fig. 8.
(A) Caspase 3 activity of cells in control (ctrl), 0.2 mM palmitate (0.2-P), 0.4 mM palmitate
(0.4-P), 0.7 mM pamitate (0.7-P), 0.7 mM oleate (0.7-O) and 0.7 mM linoleate (0.7-L) without
(w/o) or with (w/) FI for 24 hrs (n=4). (B) Apoptotic and necrotic labeling by PI (propidium
iodide) and Alexa Fluor-488 conjugated annexin V for cells in control (ctrl) and 0.7 mM
palmitatate (P) in the absence or presence of FI and/or 10 μM pan-caspase inhibitor Z-VAD-
FMK (ZVAD) for 24 hrs. *Early apoptotic cells:* PI⁻ annexin V⁺ cells; *late apoptotic cells*:
PI⁺ annexin V⁺ cells; *necrotic cells*: PI⁺ annexin V⁻ cells (n=3). *: $p<0.05$; **: $p<0.01$; ***:
$p<0.001$.
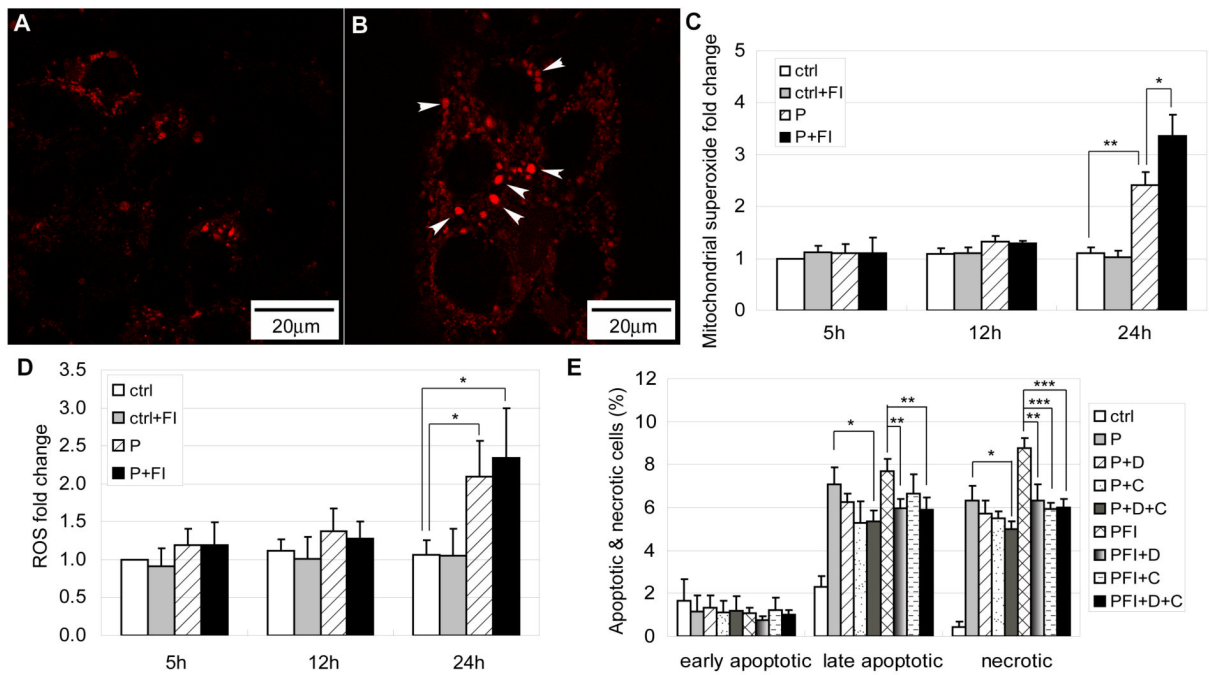
Fig. 9.
(A) Mitochondrial superoxide labeling for cells in control and (B) cells treated with 0.7 mM palmitate for 24 hrs. Arrow heads denotes short and disconnected mitochondria which have higher superoxide levels (n=3). (C) Mitochondrial superoxide levels fold change for cells in control and 0.7 mM palmitate without (w/o) or with (w/) 10 μM forskolin and 100 μM IBMX (FI) for 5 hrs, 12 hrs and 24 hrs (n=4). (D) Cellular ROS levels fold change for cells in control and 0.7 mM palmitate without (w/o) or with (w/) 10 μM forskolin and 100 μM IBMX (FI) for 5 hrs, 12 hrs and 24 hrs (n=3). (E) Apoptotic and necrotic labeling by PI (propidium iodide) and Alexa Fluor-488 conjugated annexin V for cells in control, 0.7 mM palmitate (P) and 0.7 mM palmitate supplemented with 10 μM forskolin and 100 μM IBMX (FI) in the presence of ROS inhibitors (n=3). D: hydroxyl radical inhibitor DMU; CA: hydrogen peroxide inhibitor catalase. *: p<0.05; **: p<0.01; ***: p<0.001.